This article has been accepted for publication in a future issue of this journal, but has not been fully edited. Content may change prior to final publication. Citation information: DOI 10.1109/JESTPE.2019.2942034, IEEE Journal of Emerging and Selected Topics in Power Electronics

Modelling Single-Wire Capacitive Power Transfer System with Strong Coupling to Ground

Lixiang Jackie Zou, *Student Member, IEEE*, Qi Zhu, *Student Member, IEEE*, C.W.Van Neste, *Member, IEEE*, and Aiguo Patrick Hu, *Senior Member, IEEE*

***Abstract*—This paper presents the modelling of a single-wire Capacitive Power Transfer (CPT) system to reveal its power transfer mechanism with strong coupling to ground. An equivalent circuit is proposed by treating the ground as a quasi-conductive medium. The parameters of the equivalent circuit model are determined, including the capacitance between the coupling plates of the CPT system, the single wire inductance and the capacitance between the wire and ground, and the ground equivalent impedance. The maximum power transfer capacity corresponding to the system's resonant frequency is analyzed using the proposed model to guide the system tuning design. A prototype single-wire CPT system is built, and CST (Computer Simulation Technology) simulation is undertaken to show the electric and magnetic field distributions, as well as the Poynting vector indicating the direction and magnitude of power flow in the system. It is shown that the output voltage and the power predicted by the theoretical model are in a good agreement with the simulation and practical results under frequency and load variations. Different length of the dangling single wire at the secondary side of the CPT system is also investigated to validate the model with different levels of ground effect.**

***Index Terms*—Wireless power transfer, capacitive power transfer, single-wire CPT system.**

I. Introduction

In recent years, there is a growing trend of using wireless power supplies to replace traditional fixed contact power supplies due to its convenience and safety. Inductive Power Transfer (IPT) technology based on magnetic coupling is currently the dominant solution for achieving Wireless Power Transfer (WPT), which has found many applications in industrial, commercial and biomedical fields such as materials handling in clean rooms, cell phone charging pad, implanted pacemaker, etc.[1-3]. However, IPT is not suitable for contactless power transfer across metal barriers or inside metal surrounding environments, and it has many practical limitations with regards to Electromagnetic Interference (EMI), physical size and power losses [4-7]. As an alternative WPT solution, Capacitive Power Transfer (CPT) based on electric field coupling has been proposed and attracted a lot of attention recently. This technology enables power transfer across metal barriers with potentially lower EMI, and reduces power losses with simpler coupling configuration. CPT systems are suitable for applications where metal objects exist between a stationary power source and a movable load, such as a charging platform for electric vehicle, mobile phones and laptops [8, 9]; applications where EMI and heating problems should be minimized, such as biomedical implants [10, 11]; or where the total coupling size needs to be minimized and integrated into an IC (Integrated Circuit) [12, 13].

Although CPT has clear advantages compared to IPT, it has not been widely adopted for WPT applications. A conventional CPT system in Fig. 1(a) requires two pairs coupling plates to form a current return path for wireless power transfer from a power source to a stationary/movable load. Due to the low permittivity of air ($\varepsilon_0 \approx 8.854 \times 10^{-12} F/m$) and normal dielectric constant materials that can be used between the coupling plates, it is difficult to obtain a high coupling capacitance within a confined size. Furthermore, the traditional CPT system with two pairs of coupling plates suffers from the coupling variations and cross coupling effects caused by misalignments, which can seriously affect the system power transfer performance [14-16].

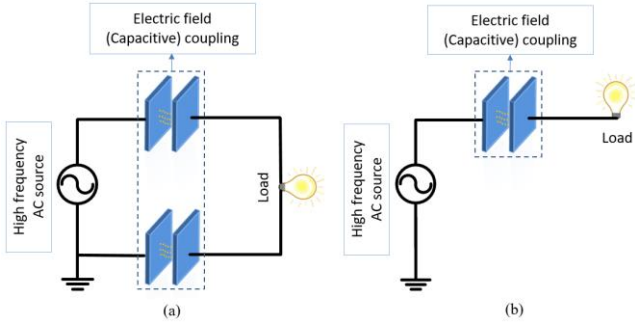

Fig. 1. Two types of CPT systems. (a) Conventional system with two pairs of coupling plates. (b) Single-wire CPT system with only one pair of coupling plates.

Recently an unexpected phenomenon was discovered from lab experiments that power can be transferred across a single pair of electric field coupling plates as illustrated in Fig. 1(b), which cannot be explained by traditional electric circuit theories as there is no closed loop for a current to flow. Such a system called single-wire CPT system. Van Neste et al. also observed a similar phenomenon for a single-wire CPT system that utilizes standing waves in the receiver, corresponding to an

Manuscript received May 29, 2019; revised July 21, 2019; accepted September 8, 2019.

Lixiang Jackie Zou and Aiguo Patrick Hu are with the Department of Electrical and Computer Engineering, University of Auckland, Auckland 1010, New Zealand (e-mail: lzou005@aucklanduni.ac.nz, a.hu@auckland.ac.nz).
Qi Zhu is with the School of Automation, Central South University, Changsha 410083, China (e-mail: csu_zhuqi@163.com).
C.W.Van Neste is with the Center for Energy Systems Research, Tennessee Tech University, Cookeville, TN 38501, USA (e-mail: cvanneste@tntech.edu)

This article has been accepted for publication in a future issue of this journal, but has not been fully edited. Content may change prior to final publication. Citation information: DOI 10.1109/JESTPE.2019.2942034, IEEE Journal of Emerging and Selected Topics in Power Electronics

explanation based on reflection theory [17], but such an explanation is incomplete as we found the system can still work without the described standing wave resonance. Two big metallic balls through a virtual self-capacitance route are used to enhance a single-wire CPT system [18], but the earth was regarded as an ideal conductor without power losses. A unipolar CPT system with two active plates/balls transfers power from transmitter to receiver by using two grounded passive plates or wire [19, 20], but the difference is that the single-wire CPT system only has one side grounded and uses an open loop dangling wire/plate on the secondary side. As a result, the current does not flow in a complete loop. In general, there is a lack in understanding the power transfer mechanism of a single-wire CPT system, so there is no systematic approach to establish accurate models for system analysis and design. However, single-wire CPT systems can be used to transfer power across metal barriers, and they demonstrated very good large coupling tolerances, which are required in many mobile wireless power transfer systems [21, 22].

This paper presents the modelling of a single-wire CPT system with strong coupling to ground. The rest of the paper is arranged as follows. Section II proposes a single-wire CPT system and establishes its equivalent circuit model. Section III determines the equivalent circuit parameters of the model. Section IV analyses the maximum power transfer capacity corresponding to the system resonant frequency and tuning to guide the system design. Finally, Section V demonstrates practical single-wire CPT prototypes and validates the theoretical and simulation results by varying the frequency, load and the wire length before the conclusion is drawn in Section VI.

II. Basic Structure of Equivalent Circuit Model

Fig. 2 shows a typical single-wire CPT configuration. A high frequency AC voltage V_s is used to drive the primary Coupling Plate 1, which can be realized by using a high frequency amplifier or a DC-AC inverter. The Coupling Plate 2 with a lumped tuning inductor L_{lump} and load R_L are connected by a dangling wire 3 with the whole secondary side left floating. The Coupling Plates 1 & 2 are two circular plates with radius r, and the dangling wire 3 is cylindrical with a total length l and radius a.

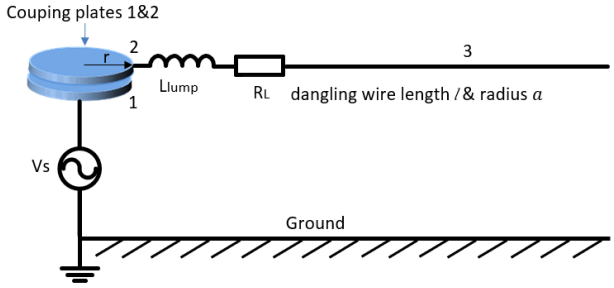

Fig. 2. The proposed single-wire CPT system.

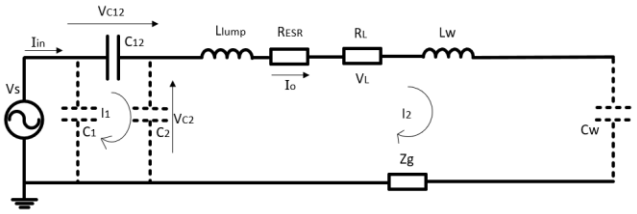

Fig. 3. The equivalent circuit model of the proposed single-wire CPT system.

Based on the practical setup, an equivalent circuit model is proposed as shown in Fig. 3. Here C_{12} is the capacitance formed between the two coupling plates, C_1 and C_2 are the capacitances between each plate (1 & 2) and the ground, respectively. L_{lump} is a lumped tuning inductor for decreasing the resonant frequency of the system, and R_{ESR} is the total equivalent series resistance of the dangling wire and the tuning inductor. L_w is the inductance of the dangling wire including the contribution from ground currents while C_w is the equivalent capacitance between the dangling wire and the ground plane. R_L is the load resistor, and Z_g is the equivalent impedance of the effective ground area. As the lower part of the source is connected to the ground, and the wire is vertical and not aligned to the ground surface, its capacitance to the ground is negligible.

III. Determining the Equivalent Circuit Parameters of the Proposed Model

A. Capacitive Coupling Plates

A capacitance is formed between two coupling plates, as well as a capacitance between each plate and ground. Considering the edge effects, the capacitance between two parallel plates can be calculated according to [23]:

$$C_{12} = [1 + 2.367b^{0.867}](\frac{\varepsilon_0 \pi r^2}{d}) \quad (0.005 \le b \le 0.5) \quad \text{or}$$

$$C_{12} = [1 + 2.564b^{0.982}](\frac{\varepsilon_0 \pi r^2}{d}) \quad (0.5 \le b \le 5.0) \quad (1)$$

where r is the radius of the plates, $\varepsilon_0 \approx 8.854 \times 10^{-12} F/m$ is the permittivity of free space and approximately that of air, d is the distance between two coupling plates, and b is the aspect ratio (b=d/2r).

As the separation distance between the coupling plates and the ground is larger compared to the size of the plates, the capacitance between each coupling plate and ground C_1 and C_2 approaches to half of their self-capacitances C_{self_plate} [24, 25].

$$C_{self\_plate} = 8\varepsilon_0 r \quad (2)$$

$$C_1 = C_2 = 4\varepsilon_0 r \quad (3)$$

B. Wire Inductance and Capacitance

A wire without insulation of total length l connected with the lumped tuning inductor L_{lump} and load R_L, will have an inductance that is influenced by the magnetic fields of the ground currents. The wire inductance between the ground L_w

This article has been accepted for publication in a future issue of this journal, but has not been fully edited. Content may change prior to final publication. Citation information: DOI 10.1109/JESTPE.2019.2942034, IEEE Journal of Emerging and Selected Topics in Power Electronics

can be determined by Eq. (4), which is based on the mirror method by assuming the ground has infinite conductivity [26].

$$L_w = \frac{\mu_0 l}{2\pi} cosh^{-1}\left(\frac{h}{a}\right) \quad (4)$$

where $\mu_0 = 4\pi \times 10^{-7} H/m$ is the permittivity of air, l and a are the total length and radius of the dangling wire respectively, and h is the distance between the wire and the ground plane.

As the separation distance between the wire and the ground is larger compared to the radius of the wire, the total equivalent capacitance between the wire and ground can be accurately modelled by using a practical 1D method as shown in equation (5). This method is usually used for an accurate extraction of interconnected parasitic capacitance found on PCB boards [27]. The first component of Eq.(5) is contributed by the wire self-capacitance, which can be determined by J. D. Jackson's correction formula for a long wire l with radius a (or equivalently, Vainshtein's formula) [28]. And the second component of Eq. (5) is contributed by the capacitance between the wire and ground, which can also be obtained by the mirror method [29].

$$C_w = 2\pi\varepsilon_0 \frac{l}{\Lambda}\left\{1 + \frac{2}{\Lambda}(1 - \ln 2) + \frac{4}{\Lambda^2}\left[1 + (1 - \ln 2)^2 - \frac{\pi^2}{12}\right] + O(1/\Lambda^3)\right\} + \frac{2\pi\varepsilon_0 l}{cosh^{-1}\left(\frac{h}{a}\right)} \quad (5)$$

where $\Lambda = 2\ln(l/a) \geq 6$, and $l/2a \geq 10$.

In this model, the wire inductance and capacitance between the wire and ground are calculated by assuming the ground has infinite conductivity. As the system operates at a resonant frequency and the lumped inductor value is large, the error introduced by the assumption can be ignored. The mirror theory has been widely used for modelling the inductance and capacitance to ground, and we found it is sufficiently accurate for determining the inductance and capacitance of the dangling wire.

C. Ground Equivalent Impedance Approximation

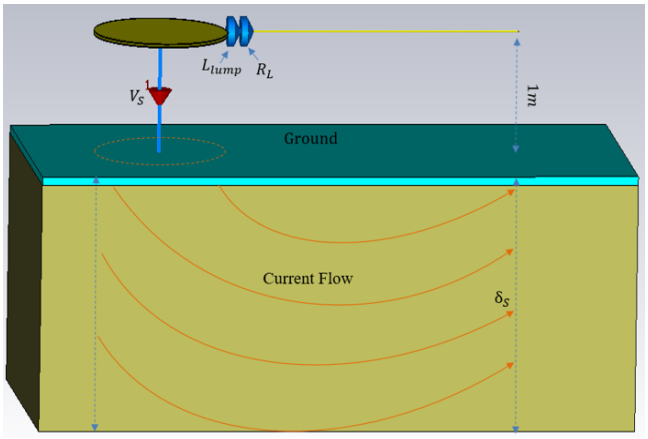

Fig. 4. Illustration of ground as a quasi-conductive path in CST.

As the equivalent circuit model of this single-wire CPT system is based on the theory that the ground is the return path, it is very important to evaluate the role of ground and estimate the equivalent impedance of the ground. In this case, the ground acts as a quasi-conductive medium as illustrated in Fig. 4 by a CST (Computer Simulation Technology) model, its conductive capability can be evaluated. Good conductivity is equivalent to $\frac{\sigma}{\omega\varepsilon} \gg 1$, while poor conductivity is equivalent to $\frac{\sigma}{\omega\varepsilon} \ll 1$ ($\varepsilon = \varepsilon_0\varepsilon_r$). The ground conductivity depends on its physical and chemical properties (texture, salinity, temperature, water content, etc.), its electrical resistivity exhibits a large range of values from 1Ωm for saline soil to 10^5 Ωm for rocks, and the relative permittivity could be about from 2 to 40 [30, 31]. To simplify the model of the ground in this case, we assume the ground is homogenously distributed and considered in two segments, concrete on top and soil underneath. Under this condition, the average ground resistivity 400Ωm with relative dielectric constant 10 is chosen for modelling the cement ground in the lab. Normally, the system operates at high frequency (1~10MHz) due to the lumped tuning inductor. In this frequency range, the ground acts as a conductor, but not as a good conductor as metal, because its conductive capability $\frac{\sigma}{\omega\varepsilon}$ is slightly larger than 1, even if the soil's relative dielectric constant is considered ($10^{-2} \leq \frac{\sigma}{\omega\varepsilon} \leq 10^2$), which can be called as a quasi-conductor [32].

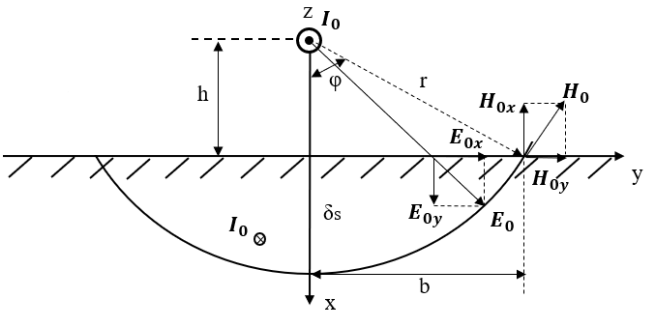

Fig. 5. Electric and magnetic fields due to the dangling wire.

As a quasi-conductor, the ground is assumed to have an infinite cross-section in conducting the current from the wire capacitance towards the voltage source. The electric and magnetic fields on the right-hand side generated by the current in the wire are shown in Fig. 5, and can be expressed by

$$\boldsymbol{E_0}(z) = (\hat{x}E_{0x} + \hat{y}E_{0y})e^{-\alpha z}e^{-j\beta z} \quad (6)$$

$$\boldsymbol{H_0}(z) = \frac{1}{\eta_c}(-\hat{x}E_{0y} + \hat{y}E_{0x})e^{-\alpha z}e^{-j\beta z} \quad (7)$$

where α, β and η_c are the attenuation constant, phase constant and intrinsic impedance of the ground, which can be determined by the operating frequency ω, the ground resistivity or conductivity ρ (σ), permittivity ε and permeability μ.

This article has been accepted for publication in a future issue of this journal, but has not been fully edited. Content may change prior to final publication. Citation information: DOI 10.1109/JESTPE.2019.2942034, IEEE Journal of Emerging and Selected Topics in Power Electronics

$$\alpha = \omega\left[\frac{\mu\varepsilon}{2}\left[\sqrt{1+(\sigma/\omega\varepsilon)^2}-1\right]\right]^{1/2} \quad (8)$$

$$\beta = \omega\left[\frac{\mu\varepsilon}{2}\left[\sqrt{1+(\sigma/\omega\varepsilon)^2}+1\right]\right]^{1/2} \quad (9)$$

$$\eta_c = \frac{\mu}{\varepsilon}[1-j(\sigma/\omega\varepsilon)]^{-1/2} = |\eta_c|e^{j\theta_\eta} \quad (10)$$

And the Poynting's vector flux over the ground surface can be expressed as:

$$S(z) = \Re e[\boldsymbol{E_0} \times \boldsymbol{H_0}^*] = \hat{z}\frac{|E_0|^2}{|\eta_c|}e^{-2\alpha z}\cos\theta_\eta \quad (11)$$

Due to the skin effect, the current density is not uniformly distributed across the infinite cross-section. Assuming the maximal real penetration value of electric filed is the skin depth $\delta_s = \frac{1}{\alpha}$, and meanwhile the angle between the electric field strength vector and the ground is φ, then the effective ground area can be calculated as:

$$A_{eff} = r \cdot l \cdot acos(h/(h+\delta_s)) \quad (12)$$

where $r = h+\delta_s$, and the l is the total dangling wire length.

Therefore, the total power through the ground path is

$$R_g|I_0|^2 = 2\int(\boldsymbol{E_0} \times \boldsymbol{H_0}^*) \cdot dA_{eff} \quad (13)$$

where the current I_0 can be determined by integrating the current density vector over the effective ground area.

$$I_0 = \int \boldsymbol{J_0} \cdot dA_{eff} = \int \sigma \boldsymbol{E_0} \cdot dA_{eff} \quad (14)$$

According to equations from (11) to (13), the total ground equivalent resistance can be obtained by:

$$R_g = \frac{2}{|I_0|^2}S \quad (15)$$

where S is the Poynting vector representing the directional energy flux along z axis.

As the system operates in a several MHz frequency range, the ground resistance is high, the reactance of the ground goes to zero and can be ignored at resonance mode, because nearly all energy is dissipated into the soil as radiated heat and/or EM waves at a resonance mode [33]. Therefore, only the equivalent ground resistance needs to be considered in the proposed model.

IV. System Resonant Frequency and Tuning Analysis Using the Proposed Model

From Fig. 3, the voltage transfer function from the output to the input of the CPT system can be expressed as equation (16). Substitute s with jω, and the voltage gain at steady state (the transfer function magnitude) can be determined as equation (17).

Let the imaginary part of the transfer function be zero, the zero-phase angle resonant frequency ω_o can be determined as:

$$\omega_o = \sqrt{\frac{C_{12}+C_2+C_w}{C_w(L_{lump}+L_w)(C_{12}+C_2)}} \quad (18)$$

The magnitude of the transfer function at the resonant frequency ω_0 can be determined as:

$$|H(j\omega_o)| = \frac{V_L}{V_s} = \frac{R_L C_{12}}{(R_L+R_{ESR}+R_g)(C_{12}+C_2)} \quad (19)$$

At the resonant frequency, the output power reaches approximately the maximum power, which can be expressed as:

$$P_{max} = \frac{{V_L}^2}{R_L} = \left[\frac{R_L C_{12}}{(R_L+R_{ESR}+R_g)(C_{12}+C_2)}\right]^2 \frac{{V_s}^2}{R_L} \quad (20)$$

In the proposed single-wire CPT system, the lumped inductor L_{lump} is added to reduce the system resonant frequency, which otherwise would be too high for practical operation because the parasitic dangling wire inductance L_w is normally very low. To tune the system to a lower resonant frequency ω_o, the lumped inductance can be determined by the following equation:

$$L_{lump} = \frac{C_{12}+C_2+C_w}{{\omega_0}^2 C_w(C_{12}+C_2)} - L_w \quad (21)$$

V. Simulation and Experimental Verification

To verify the proposed single-wire CPT system and the modelling method, CST (Computer Simulation Technology) simulation and experimental study are further carried out. Table I shows the system parameters for simulation and experiment. As the ground underneath the lab floor is concrete, the average ground resistivity of about 400Ωm and relative dielectric constant of about 10 are selected according to the previous study of the ground for system modelling. The calculated values are obtained from the equations derived in Section III and IV previously, in which the equivalent ground resistance is calculated when the system operates from 1MHz to 10MHz. The equivalent ground resistance changes with the operating frequency.

$$H(s) = \frac{V_L}{V_s} = \frac{V_{c2}}{V_s}\cdot\frac{V_L}{V_{c2}} = \frac{sR_L C_{12} C_w}{s^2 C_w(L_{lump}+L_w)(C_{12}+C_2) + s(R_L+R_{ESR}+R_g)C_w(C_{12}+C_2) + C_{12}+C_2+C_w} \quad (16)$$

$$|H(j\omega)| = \frac{\omega R_L C_{12} C_w}{\sqrt{[\omega(R_L+R_{ESR}+R_g)(C_{12}+C_2)C_w]^2 + [\omega^2 C_{12} C_w(L_{lump}+L_w) + \omega^2 C_2 C_w(L_{lump}+L_w) - C_{12} - C_2 - C_w]^2}} \quad (17)$$

This article has been accepted for publication in a future issue of this journal, but has not been fully edited. Content may change prior to final publication. Citation information: DOI 10.1109/JESTPE.2019.2942034, IEEE Journal of Emerging and Selected Topics in Power Electronics

TABLE I
SYSTEM PARAMETERS FOR SIMULATION AND EXPERIMENT

Symbol	Parameter	Value
V_s	Input voltage (Amplitude/Peak value)	100 V
r	Coupling plates radius	10 cm
d'	Coupling plates thickness	1 mm
d	Distance between coupling plates	3 mm
l	Total wire length including components length (copper)	0.43 m
a	Wire radius	1 mm
h	Height above the ground	1 m
L_{lump}	Lumped tuning inductor	470 μH
R_{ESR}	Total ESR of lumped tuning inductor and wire	6.5 Ω
f	Frequency range	1~10 MHz
R_L	Load	500 Ω/LED
C_{12}	Capacitance between two coupling plates	98.47 pF (calculated)
C_w	Equivalent capacitance between the wire and ground	5.26 pF (calculated)
L_w	Wire inductance	0.608 μH (calculated)
C_1	Capacitance between coupling plate 1 and ground	3.54 pF (calculated)
C_2	Capacitance between coupling plate 2 and ground	3.54 pF (calculated)
R_g	Equivalent ground resistance range	628.75~616.60 Ω (calculated from1-10MHz)

The simulation study is undertaken in a frequency domain from 1MHz to 10MHz in CST Microwave studio. Since the system physical dimensions are much smaller than the free space wavelength λ0 of the resonant operating frequency (smaller than 0.1 λ0), so this single-wire CPT system falls under quasi-static near field region, and the wire can be simply modelled in terms of a lumped-element circuit model as illustrated in Fig. 3. To simplify the system simulation, an ac input voltage V_s is directly applied on the primary coupling plate. The electric field, the magnetic field and the power flow distributions at the resonant frequency 3.3MHz are shown as in Fig. 6. As can be seen from the Fig. 6 (a) and (b), the ac voltage source generates strong electric field **E(t)** and weak magnetic field **H(t)** between two coupling plates. The high electric field occurs around the surface of the secondary plate and along the dangling wire. According to the IEEE C95.1 Standard, the human exposure of electric fields is 830/f (V/m) between 3-30MHz. In a practical system the maximum electric field people can approach can be reduced by shielding or adding an insulation layer.These coupled **E(t)** and **H(t)** fields distribute along the dangling wire, which results in a voltage difference and displacement/leakage current between the wire and the ground. As the wire length is much shorter than the wavelength (about 91m at 3.3MHz), the current in the wire is almost constant except for zero at the end as shown in Fig. 7. This is similar to an open-circuited short transmission line. The difference is only one line is available and a ground plane is involved. The current flow into the ground of the proposed CPT system is low, and the earth effective area is large, so the current density in the effective area is much lower compared to the current density in the wire. The current is distributed in the ground rather than flows in a closed loop, and its actual distribution and effect on the safety and EMI (Electromagnetic Interference) needs to be studied further in the future.

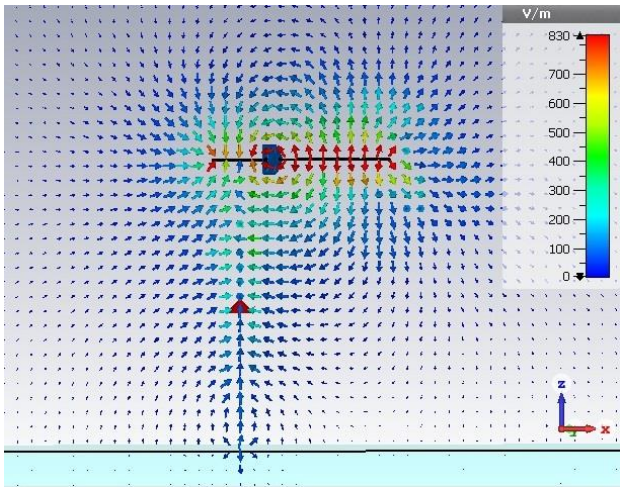

(a)

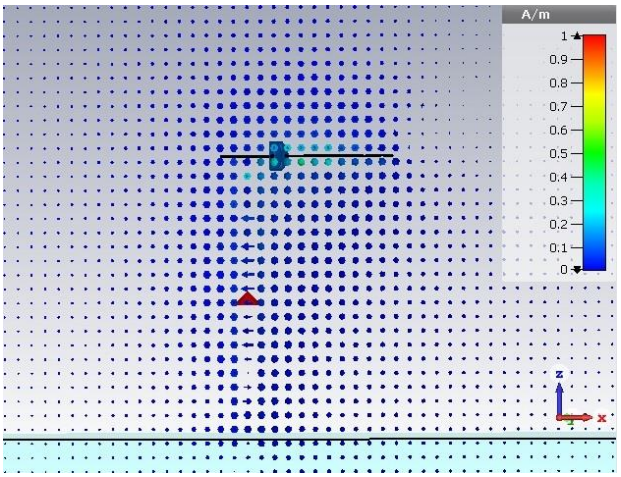

(b)

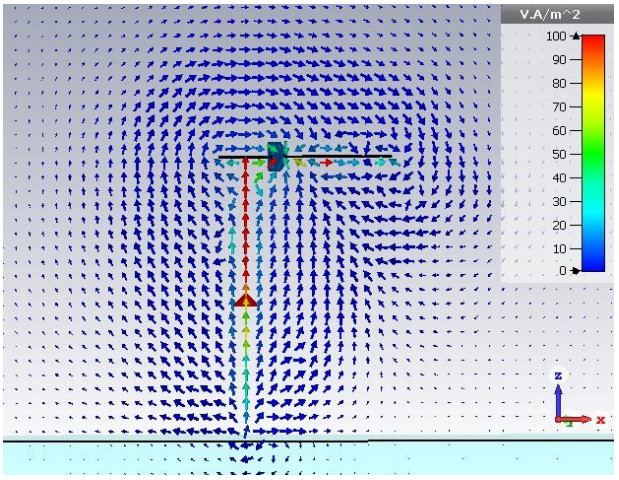

(c)

Fig.6. (a) A 2D view of electric field distribution. (b) A 2D view of magnetic field distribution. (c) A 2D view of Poynting vector showing power flow distribution.

This article has been accepted for publication in a future issue of this journal, but has not been fully edited. Content may change prior to final publication. Citation information: DOI 10.1109/JESTPE.2019.2942034, IEEE Journal of Emerging and Selected Topics in Power Electronics

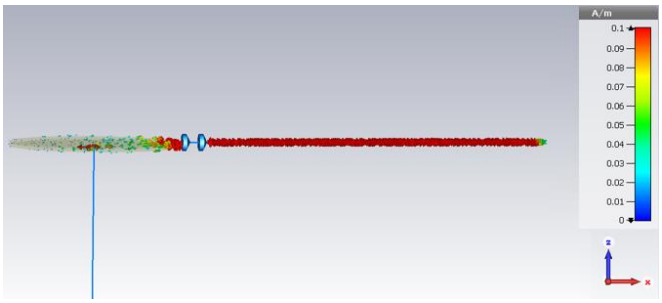

Fig. 7. A 3D view of current density distribution.

A prototype was built and shown in Fig. 8. A high frequency power amplifier (Agitek ATA-122D) is used as a variable frequency power source, which is connected to an LCLC tuning circuit to provide a constant input ac voltage V_s with an amplitude of 100V.

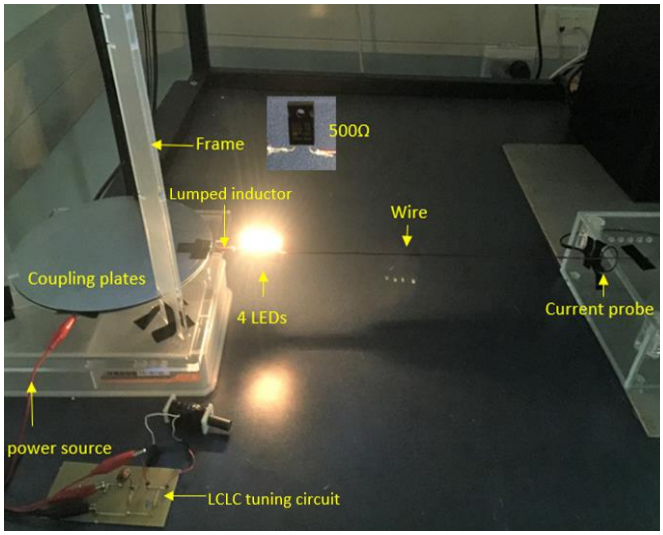

Fig. 8. A prototype of single-wire CPT system with LEDs and 500Ω.

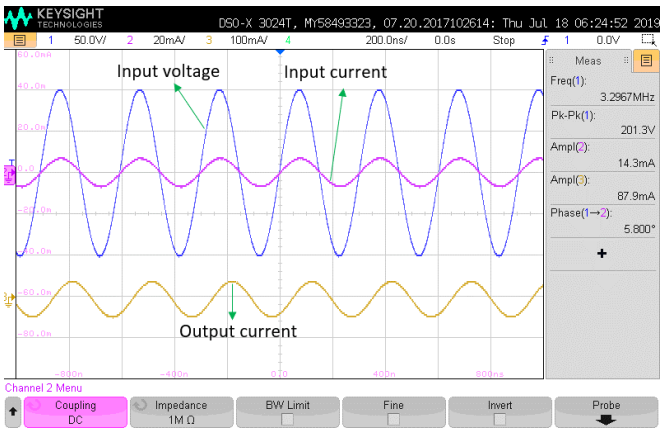

Fig. 9. Input voltage, input current and output current waveforms.

Firstly, the functionality of the system is tested by using an LED lamp as shown in Fig. 8, and the typical waveforms of the input voltage V_s, input current I_{in} and the output current I_o are measured in Fig. 9 when the system achieves the approximate maximum power on the LED lamp. The result shows the input voltage and current are approximately in phase, with an actual phase difference of 5.8 degrees. This is in consistent with the theoretical result of 0 degree when the system operates at resonant frequency. It also can be seen that the output current in the wire is much higher than the input current, because the system is resonant, and the current in the resonant loop could be higher than the input current. Since the coupling plates and wire capacitances to the ground (C_1, C_2 and C_w) are very small, the resonant current through those capacitors are very small, so most resonant current stay in the dangling wire.

An optometer is used to measure the output power of the LED lamp without direct contact, yielding a total output power of 3.6W with 201V (peak-peak value) input voltage. The system efficiency from the AC source to the final resistive load is 35%. The LED load can be placed at any position of the dangling wire except at the terminal of the wire, because the current is zero at the end of the wire. As the wire length is much shorter than the wavelength (about 91m at 3.3MHz), the current in the wire is almost constant except at the end, so the power to LED stays more or less the same along the wire, but it becomes zero at the farther end.

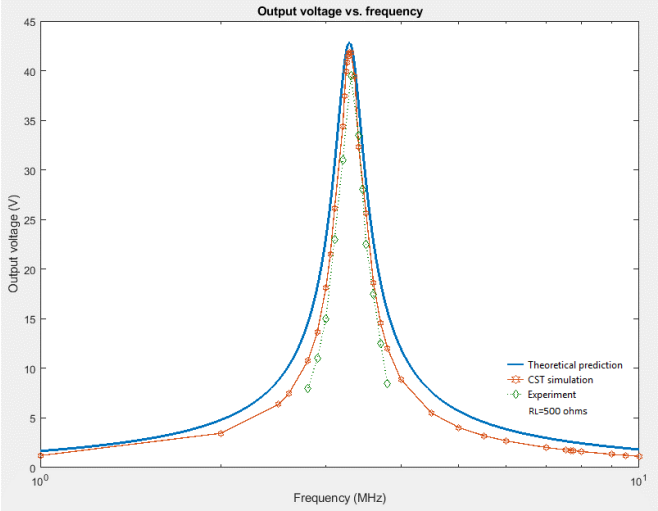

Fig. 10. Output voltage vs. frequency variation at constant load of 500Ω.

The effect of the frequency variation on the system performance is studied at a constant load of 500Ω. A current probe is used to measure the current through the dangling wire to minimize the effect of measurement equipment on the result, then the load voltage across the resistor is calculated. Fig. 10 shows the simulation, experimental and theoretical results are plotted against frequency variation in logarithm scale from 1MHz to 10MHz at a constant load of 500 Ω. The CST simulation results show the maximum output voltage occurs at the frequency of 3.3MHz. Therefore, the operating frequency range from 2.8MHz to 3.8MHz was chosen. This also made the experimental results more accurate as the output current outside of this frequency range was low and not easy to measure accurately. As can be seen from the Fig. 10, the maximum output voltages predicted by the theoretical model and CST simulation occur at 3.28MHz and 3.3MHz respectively, while

This article has been accepted for publication in a future issue of this journal, but has not been fully edited. Content may change prior to final publication. Citation information: DOI 10.1109/JESTPE.2019.2942034, IEEE Journal of Emerging and Selected Topics in Power Electronics

the experimental maximum output voltage occurs around 3.3MHz as well. Comparing these three results from the theoretical prediction, simulation and experiment in the frequency range of 1~10MHz, we can see that the proposed equivalent circuit model is able to predict the output voltage of this single-wire CPT system with reasonable accuracy without consideration of the reactance component of the ground.

Different loads of 200 Ω and 600 Ω are tested to further investigate the influence of the load variation on the output voltage of the system. Fig.11 shows the output voltages under different load conditions against frequency variation in a linear scale when the system setup maintains the same values given in Table I. The maximum output voltages for the different load values all occur around the resonant frequency of 3.3MHz. It is noteworthy that the output voltages and the bandwidth are positive in proportion to the load values, which is reasonable for this resonant system, because the quality factor Q decreases as the load value increases. The lower the Q, the bigger the bandwidth, and vice versa.

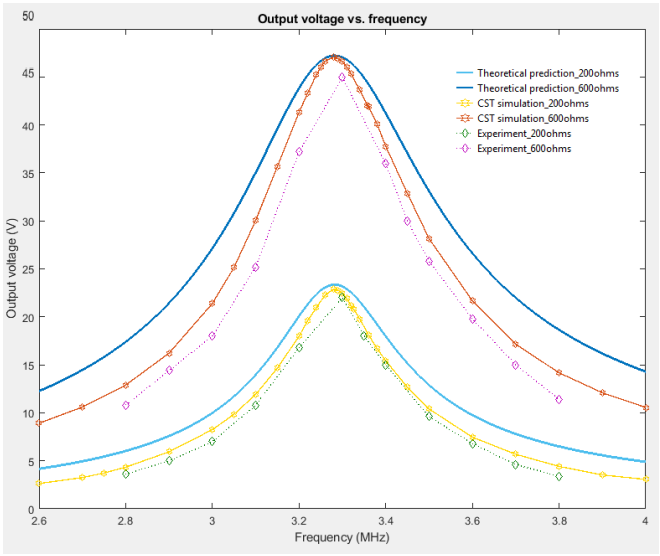

Fig. 11. Output voltage vs. frequency variation with 200Ω and 600Ω.

The wire with different lengths of 50cm and 60cm are modelled, simulated, and tested to validate the theoretical model with different levels of ground effect. All of parameters are same as shown in Table I, except for the dangling wire length, which means the wire inductance, capacitance and the equivalent ground resistance will change too. Table II and Fig. 12 show the results from theoretical model, simulation and experiment when the dangling wire length is varied. The maximum output voltages calculated from the theoretical model are approximate to the simulation results when the ground resistivity and relative permittivity are set with 400Ωm and 10 respectively. But the experimental output results are little bit lower than the theoretical ones as the actual ground resistivity and relative permittivity may be lower than the assumed values. Different ground resistivity and relative permittivity will result in different output voltage. Moreover, based on the proposed theoretical model, the wire inductance, capacitance and the equivalent ground resistance are replaced with an inductor, capacitor and resistor in LTspice, and their values are the same as the calculated values, the output voltages on the load are quite close to the theoretical values under the resonant frequency, which further verifies that the theoretical model can predict the output power and ground loss of the proposed single-wire CPT system.

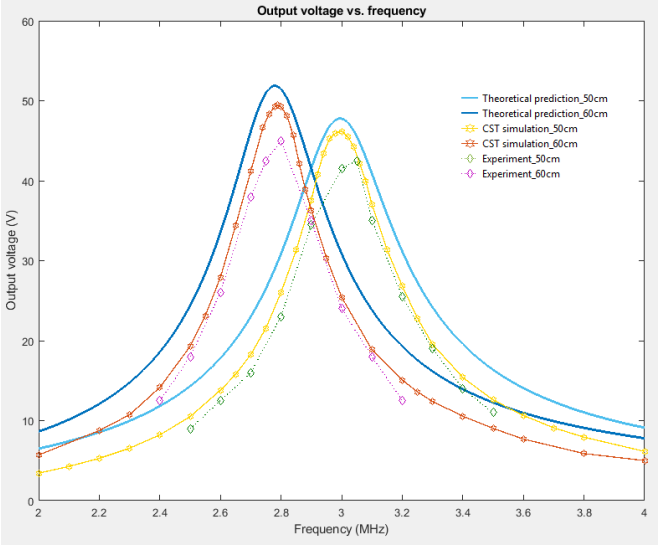

Fig. 12. Output voltage vs. frequency variation with different wire length.

TABLE II
RESULTS FROM THEORETICAL MODEL, SIMULATION AND EXPERIMENT

Parameters	**Case I**	**Case II**	**Case III**
Total wire length *l* including components length	0.43m	0.53m	0.63m
Theoretical results			
Equivalent capacitance between wire and ground C_w	5.26 pF	6.38 pF	7.48 pF
Wire inductance L_w	0.608 μH	0.806 μH	0.958 μH
Equivalent ground resistance (1~10MHz) R_g	628.75~616.60 Ω	510.12~500.26 Ω	429.15~420.85 Ω
Resonant frequency f	3.29 MHz	3 MHz	2.78 MHz
Maximum output voltage V_{Lmax} (Amplitude/Peak)	42.83V	47.78V	51.87V
CST simulation results			
Resonant frequency f	3.3 MHz	3 MHz	2.79 MHz
Maximum output voltage V_{Lmax} (Amplitude/Peak)	41.84V	46.18V	49.44V
Experiment results			
Resonant frequency f	3.3 MHz	3.05 MHz	2.8 MHz
Maximum output voltage V_{Lmax} (Amplitude/Peak)	39.5V	42.5V	45V

VI. Conclusion

This paper has developed an equivalent circuit model to explain the working principle of a typical single-wire CPT system. The effect of the ground on the CPT system is considered by treating it as a quasi-conductive medium. The capacitance between the coupling plates, wire inductance and capacitance between the wire and ground, equivalent ground resistance, and the methods to determining these parameters are provided. The system voltage transfer function and the resonant frequency are analyzed using the proposed model, and the inductance needed for tuning the system is determined. A prototype single-wire CPT system was built, and the system resonant frequency and the output voltage were evaluated under frequency, load and the dangling wire length variations. Both the CST simulation results and experimental measurements have shown that the proposed equivalent circuit model can be used to predict the performance of the single-wire CPT system with reasonable accuracy.

References

[1] G. A. Covic, G. Elliott, O. H. Stielau, and R. M. G. J. T. Boys, "The design of a contact-less energy transfer system for a people mover system," presented at the Power System Technology, 2000. Proceedings. PowerCon 2000. International Conference on 2000.

[2] A. P. Hu, "Selected Resonant Converters for IPT Power Supplies," PhD thesis, Department of Electrical and Computer Engineering, University of Auckland, Auckland, 2001.

[3] H. Matsuki, "Energy transfer system utilizing amorphous wires for implantable medical devices," *IEEE Transactions on Magnetics*, vol. 31, pp. 1276-1282, 1995.

[4] C. Liu, "Fundamental Study On Capacitive Coupled Power Transfer Technology," PhD thesis, Department of Electrical and Computer Engineering, University of Auckland, Auckland, 2011.

[5] W. R. Wilson, l. G. C. Robertson, J. L. Zwi, and B. V. Dawson, "Health Effects of Sinusoidal 10 kHz Magnetic Fields," 20 December 1993.

[6] International Commission on Non-Ionizing Radiation Protection, "Guidelines for limiting exposure to time-varying electric, magnetic, and electromagnetic fields (up to 300GHz)," Health Physics1998.

[7] Z. Qingping, "Problems on demonstration of the electric field producing the magnetic field" in *ICMMT'98. 1998 International Conference on Microwave and Millimeter Wave Technology. Proceedings* 1998, pp. pp.602-606.

[8] F. Lu, H. Zhuang, and C. Mi, "A Two-Plate Capacitive Wireless Power Transfer System for Electric Vehicle Charging Applications," *IEEE Transactions on Power Electronics*, vol. 33, pp. 964 - 969, 2018.

[9] C. Liu, A. P. Hu, B. Wang, and N.-K. C. Nair, "A Capacitively Coupled Contactless Matrix Charging Platform With Soft Switched Transformer Control," *IEEE Transactions on Industrial Electronics*, vol. 60, pp. 249-260, 2013.

[10] K. V. T. Piipponen, R. Sepponen, and P. Eskelinen, "A Biosignal Instrumentation System Using Capacitive Coupling for Power and Signal Isolation," *IEEE Transactions on Biomedical Engineering*, vol. 54, pp. 1822 - 1828, 2007.

[11] H. Zheng, K. Tnay, N. Alami, and A. P. Hu, "Contactless Power Couplers for Respiratory Devices," presented at the Mechatronics and Embedded Systems and Applications (MESA), 2010 IEEE/ASME International Conference on, 2010.

[12] E. Culurciello and A. G. Andreou, "Capacitive Inter-Chip Data and Power Transfer for 3-D VLSI," *IEEE Transactions on Circuits and Systems II: Express Briefs*, vol. 53, pp. 1348-1352, 2006.

[13] A. M. Sodagar and P. Amiri, "Capacitive coupling for power and data telemetry to implantable biomedical microsystems," presented at the 2009 4th International IEEE/EMBS Conference on Neural Engineering, 2--9.

[14] A. Kumar, S. Pervaiz, C.-K. Chang, S. Korhummel, Z. Popovic, and K. K. Afridi, "Investigation of power transfer density enhancement in large air-gap capacitive wireless power transfer systems," presented at the Wireless Power Transfer Conference (WPTC), 2015.

[15] L. Huang and A. P. Hu, "Defining the mutual coupling of capacitive power transfer for wireless power transfer," *Electronics Letters*, vol. 51, pp. 1806-1807, 2015.

[16] C. Liu, A. P. Hu, and M. Budhia, "A Generalized Coupling Model for Capacitive Power Transfer Systems," in *IECON 2010 - 36th Annual Conference on IEEE Industrial Electronics Society*, 2010, pp. 274-279.

[17] C. W. V. Neste, J. E. Hawk, A. Phani, J. A. J. Backs, R. Hull, T. Abraham, *et al.*, "Single-contact transmission for the quasi-wireless delivery of power over large surfaces," *Wireless Power Transfer*, vol. 1, pp. 75-82, 2014.

[18] X. Gao, H. Zhou, W. Hu, Q. Deng, G.-P. Liu, and J. Lai, "Capacitive power transfer through virtual self-capacitance route," *IET Power Electronics*, vol. 11, pp. 1110 - 1118, 2018.

[19] F. Lu, H. Zhang, and C. Mi, "A Two-Plate Capacitive Wireless Power Transfer System for Electric Vehicle Charging Applications" *IEEE Transactions on Power Electronics*, vol. 33, pp. 964 - 969, 2018.

[20] X. Shu and B. Zhang, "Single-Wire Electric-Field Coupling Power Transmission Using Nonlinear Parity-Time-Symmetric Model with Coupled-Mode Theory," *Energies*, vol. 11(3), 2018.

[21] L. J. Z. A. P. H. Y.-g. Su, "A single-wire capacitive power transfer system with large coupling alignment tolerance," presented at the 2017 IEEE PELS Workshop on Emerging Technologies: Wireless Power Transfer (WoW), 2017.

[22] L. J. Zou and A. P. Hu, "A Contactless Single-Wire CPT (Capacitive Power Transfer) Power Supply for Driving a Variable Message Sign," presented at the 2018 IEEE PELS Workshop on Emerging Technologies: Wireless Power Transfer (Wow), 2018.

[23] H. Nishiyama and M. Nakamura, "Form and capacitance of parallel-plate capacitor," *IEEE Transactions on Components, Packaging, and Manufacturing Technology*, vol. 17, pp. 477 - 484, 1994.

[24] T. M. Minteer, "The many capacitance terms of two parallel discs in free space," *European Journal of Physics*, vol. 35, pp. pp.1-15, 2014.

[25] S. N. Makarov, G. M. Noetscher, and A. Nazarian, *Low-Frequency Electromagnetic Modeling for Electrical and Biological Systems Using MATLAB*: Wiley, 2015.

[26] I. C. D. P. D. Toader, "Calculation of inductance of conductors for overhead power lines " presented at the 2011 IEEE EUROCON - International Conference on Computer as a Tool, Lisbon, Portugal, 2011.

[27] W. Yu and Z. Wang, "Capacitance Extraction," *Encyclopedia of RF and microwave engineering. Wiley, Hoboken*, pp. 565-576, 2005.

[28] J. D. Jackson, "Charge density on thin straight wire, revisited," *American Journal of Physics*, vol. 68, pp. pp.789-799, 2000.

[29] W. Buller and B. Wilson, "Measurement and Modeling Mutual Capacitance of Electrical Wiring and Humans," *IEEE Transactions on Instrumentation and Measurement* vol. 55, pp. 1519 - 1522, 2006.

[30] J. Cihlar and F. Ulaby, " Dielectric properties of soils as a function of moisture content," University of Kansas Center for Research, Lawrence,1974.

[31] A. Samoue¨lian, I. Cousin, A. Tabbaghc, A. Bruandd, and G. Richard, "Electrical resistivity survey in soil science a review," *ScienceDirect*, vol. 83, pp. 173-193, 2005.

[32] F. T. Ulaby, *Fundamentals of Applied Electromagnetics*: Prentice Hall, 1994.

[33] C. Van Neste, R. Hull, J. Hawk, A. Phani, and T. Thundat, "Electrical excitation of the local earth for resonant, wireless energy transfer," *Wireless Power Transfer*, vol. 3, pp. 117-125, 2016.

Lixiang Jackie Zou received the B.E. (Hons.) and M.E. (Hons.) degrees from the Electrical and Computer Department, University of Auckland, Auckland, New Zealand, in 2009 and 2012, respectively. She is currently working towards the Ph.D. degree in the Electrical and Computer Department, University of Auckland. Her current research interests include inductive power transfer, capacitive power transfer and electromagnetic field analysis.

Qi Zhu was born in Anhui Province, China, in 1993. He received the B.S. degree in electrical engineering and automation from Central South University, Changsha, China, in 2014, where he is currently working toward the Ph.D. degree in electrical engineering. From December 2017 till now, he is a joint Ph.D. student founded by China Scholarship Council at the University of Auckland, Auckland, New Zealand. His main research interest is Wireless Power Transfer, including both Inductive Power Transfer and Capacitive Power Transfer.

Charles W. Van Neste is a Research Assistant Professor working in the Center for Energy Systems Research at Tennessee Tech University. He obtained his Ph.D. degree in Electrical Engineering from Tennessee Tech in 2009. Dr. Van Neste's primary research involves alternative forms of energy transmission and generation. His areas of expertise include wireless and quasi-wireless power transfer, power electronics, and instrumentation.

Aiguo Patrick Hu received the B.E. and M.E. degrees from Xian JiaoTong University, Xian, China, in 1985 and 1988, respectively, and the Ph.D. degree from the University of Auckland, Auckland, New Zealand, in 2001, He was a Lecturer, a Director of China Italy Cooperative Technical Training Center, Xian, and the General Manager of a technical development company. Funded by Asian2000 Foundation, he was with the National University of Singapore for a semester as an exchange Postdoctoral Research Fellow. He is currently in the Department of Electrical and Computer Engineering, University of Auckland, and also the Head of Research of PowerbyProxi, Ltd. He holds 15 patents in wireless/contactless power transfer and microcomputer control technologies, published more than 200 peer-reviewed journal and conference papers, authored a monograph on wireless inductive power transfer technology, and contributed four book chapters.